Homeostasis established by coordination of subcellular compartment plasticity improves spike encoding

Na Chen, Xin Chen and Jin-Hui Wang*

State Key Labs for Macrobiomolecules and Brain and Cognitive Sciences, Institute of Biophysics, Chinese Academy of Sciences, Beijing 100101, The People's Republic of China

*Author for correspondence (e-mail: jhw@sun5.ibp.ac.cn)

Accepted 24 December 2007
Journal of Cell Science 121, 2961-2971 Published by The Company of Biologists 2008
doi:10.1242/jcs.022368

Summary

Homeostasis in cells maintains their survival and functions. The plasticity at neurons and synapses may destabilize their signal encoding. The rapid recovery of cellular homeostasis is needed to secure the precise and reliable encoding of neural signals necessary for well-organized behaviors. We report a homeostatic process that is rapidly established through Ca^{2+}-induced coordination of functional plasticity among subcellular compartments. An elevation of cytoplasmic Ca^{2+} levels raises the threshold potentials and refractory periods of somatic spikes, and strengthens the signal transmission at glutamatergic and GABAergic synapses, in which synaptic potentiation shortens refractory periods and lowers threshold potentials. Ca^{2+} signals also induce an inverse change of membrane excitability at the soma versus the axon. The integrative effect of Ca^{2+}-induced plasticity among the subcellular compartments is homeostatic in nature, because it stabilizes neuronal activities and improves spike timing precision. Our study of neuronal homeostasis that is fulfilled by rapidly coordinating subcellular compartments to improve neuronal encoding sheds light on exploring homeostatic mechanisms in other cell types.

Supplementary material available online at
http://jcs.biologists.org/cgi/content/full/121/17/2961/DC1

Key words: Homeostatic plasticity, Neuron, Synapse, Calcium, Excitability, Threshold potential, Refractory period, Action potential

Introduction

Cells in living organisms are able to maintain the stability of their functions by homeostatic mechanisms under physiological conditions. In the central nervous system, neurons and synapses encode signals reliably and precisely to control well-organized behavior. However, these neural units undergo refinement during learning and development, and their plasticity might destabilize the functions of the neural network (Turrigiano and Nelson, 2004). How are the functions of these neural units regulated homeostatically in order to preserve the triggers that are needed to establish the functional stability of neural networks in a precise and reliable manner?

Homeostatic changes in neuronal function have been observed after pharmacological or genetic manipulation (Burrone and Murthy, 2003; Turrigiano and Nelson, 2004). Neuronal excitability increases upon removal of tetrodotoxin (TTX), an antagonist of voltage-gated Na^+ channels. The density of AMPA receptors rises after addition of their antagonist CNQX to cultured hippocampal neurons. The increase and recovery in spiking rate occur sequentially when GABAergic synapses are blocked. Neuronal excitability decreases and then recovers when K^+ channels are overexpressed (Ramakers et al., 1990; Van Den Pol et al., 1996; Desai et al., 1999a; Desai et al., 1999b). These examples of slow-onset homeostasis might play a role in the body's management of chronic disorders and in adaptation to a changing environment. However, many types of activity-dependent plasticity of neural functions onset rapidly, and homeostatic regulation needs to be instigated quickly to counteract any destabilization in function of the neuronal network. To date, no study addresses acute mechanisms for neuronal homeostasis. It is also not known whether the homeostatic mechanisms take place in subcellular compartments, such as in the soma and axon, or between the synapses and neuron. This fast-onset neuronal homeostasis, if it exists, must quickly and efficiently rebalance the neuronal functions without the need to wait for gene expression.

Little is known about the molecular mechanisms underlying neuronal homeostasis, although it has been shown that glutamate and GABA receptors, voltage-gated Na^+ and K^+ channels, brain-derived neurotrophic factor and calmodulin-dependent protein kinase-α and -β, are all involved (Desai et al., 1999a; Desai et al., 1999b; Burrone et al., 2002; Thiagarajan et al., 2002; Ehlers, 2003; Perez-Otano and Ehlers, 2005). As these molecules are influenced by Ca^{2+} (Kennedy, 1989; Miller, 1991; Berridge, 1998; Montell, 2005), intracellular Ca^{2+} is likely to be a primary coordinator for the rapid emergence of neural homeostasis. We have therefore investigated whether a counterbalance exists among synaptic, somatic and axonal activities, and whether cytoplasmic Ca^{2+} coordinates this counterbalance. For this, we elevated the levels of cytoplasmic Ca^{2+} by using adenophostin-A, a potent and specific agonist of inositol (1,4,5)-trisphosphate receptors (IP_3Rs), to evoke Ca^{2+} release from intracellular stores (Takahashi et al., 1994; Delisle et al., 1997; Correa et al., 2001) and applied modulators of Ca^{2+}-signaling pathways via whole-cell perfusion into pyramidal neurons in cortical slices. The elucidation of how neuronal homeostasis is maintained will provide insight for addressing homeostatic mechanisms in other cell types.

Results

We used cortical pyramidal neurons as a model to investigate homeostatic processes that maintain stable cellular functions. Intense activity of synapses or neurons induces their functional plasticity (Bliss and Gardner-Medwin, 1973; Aizenmann and Linden, 2000; Zhang et al., 2004), which may call for immediate homeostatic changes in neighboring compartments to keep neuronal function stable. This hypothesis predicts that the influence of plasticity at excitatory synapses on neuronal activities is counteracted by changes at inhibitory synapses, and that somatic strengthening is neutralized by a decrease of axonal excitability or vice versa. In addition to testing this hypothesis, we investigated how the changes in cytoplasmic Ca^{2+} levels reset the functionality of subcellular compartments in a coordinated manner to secure precise neuronal encoding.

Intracellular Ca^{2+} enhances the strength of glutamatergic and GABAergic synapses

Cortical pyramidal neurons receive glutamatergic synaptic inputs at dendrites and GABAergic inputs mainly at proximal dendrites and the soma (Freund and Buzsaki, 1996). Intracellular Ca^{2+} modulates the function of both glutamatergic and GABAergic synapses (Lyncy et al., 1983; Neveu and Zucker, 1996; Wang and Stelzer, 1996). To better understand how cytoplasmic Ca^{2+} influences these two types of synapses in a coordinated manner, we elevated intracellular Ca^{2+} levels by infusing adenophostin-A (100 nM in the recording pipette, Fig. 1) into pyramidal neurons to trigger Ca^{2+} release from IP_3-sensitive intracellular stores (Takahashi et al., 1994; Delisle et al., 1997; Correa et al., 2001).

The effects of raising cytoplasmic Ca^{2+} levels on glutamatergic and GABAergic synaptic transmission are shown in Fig. 2. Adenophostin-A enhanced excitatory postsynaptic currents (EPSCs) from 101.3±12% (○ in Fig. 2A) to 243.8±17.2% (● in Fig. 2A) after 30 minutes (P<0.001, n=19). Compared with the control (103±9.2%, ○ in Fig. 2B), adenophostin-A raised inhibitory postsynaptic currents (IPSCs) to 189.5±9.8% (P<0.001, n=14; ● in Fig. 2B). These results indicate that the elevation of intracellular Ca^{2+} levels strengthens glutamatergic synapses more than GABAergic synapses.

The propagation of EPSCs from the dendrite towards the soma is shunted by inhibitory synaptic activity. Ca^{2+}-induced potentiation predominantly at excitatory synapses (Fig. 2) means that potentiation at inhibitory synapses is unable to completely counteract the effect of excitatory synaptic potentiation on neuronal activity. A net increase in excitatory component makes neurons more excitable, which may break down previous homeostasis and destabilize neuronal functions. This, therefore, raises the question of whether cytoplasmic Ca^{2+} regulates intrinsic somatic properties in order to counterbalance this net increase in excitatory component and to correct the destabilization.

Neuronal spike capacity and intrinsic properties are downregulated by raising cytoplasmic Ca^{2+}

The influence of elevated cytoplasmic [Ca^{2+}] on the programming of sequential spikes was examined by infusing adenophostin-A (100 nM) under current-clamp recording (Fig. 3). Spike capacity is denoted inversely as inter-spike interval (ISI), and spike-timing precision is represented as the standard deviation of spike timing (SDST) (Chen et al., 2006a). Compared with the initial control value, adenophostin-A prolonged ISI (Fig. 3A,B). The values of ISI_1, ISI_2, ISI_3 and ISI_4 were 21±1.8, 37.9±1.62, 44.1±1.77 and 45.93±1.9 mseconds, respectively, under control conditions (Fig. 3C, △), and 27.57±1.62, 43.72±1.9, 49.96±2.1 and 51.9±2.14 mseconds after adenophostin-A infusion (Fig. 3C, ▲). ISI values for corresponding spikes under both conditions were statistically different (P<0.01, n=12). The elevated cytoplasmic [Ca^{2+}] did not affect spike timing because there was no statistical difference in the values for $SDST_1$ to $SDST_5$ under initial control (Fig. 3D, open symbols) and adenophostin-A infusions (filled symbols in Fig. 3D; P=0.87, n=12). These data indicate that the elevation of intracellular Ca^{2+} lowers the neuronal capacity to fire sequential spikes.

We examined whether the decrease of spike capacity by raising intracellular [Ca^{2+}] is due to an increase in threshold potentials (V_{ts}) and/or refractory period (RP), because the spike capacity is controlled by V_{ts} and RP (Chen et al., 2006b; Chen et al., 2006c). When measuring absolute RP under different stimulus intensities, we found a linear correlation between absolute RPs and normalized stimuli (Fig. 4B). As the slopes are steeper in the absolute RP_3 (–10.4 and –12.6) than the absolute RP_1 (–3.1 and –3.4), an increase in input intensity reduces the absolute RP mainly in the late phase of sequential spikes. Compared with the control (blue curve in Fig. 4A), an elevation of cytoplasmic [Ca^{2+}] prolongs the absolute RP subsequent to spike three (red curve in Fig. 4A). Fig. 4B shows the values of the absolute RP_1 and absolute RP_3 in control (open symbols) and after

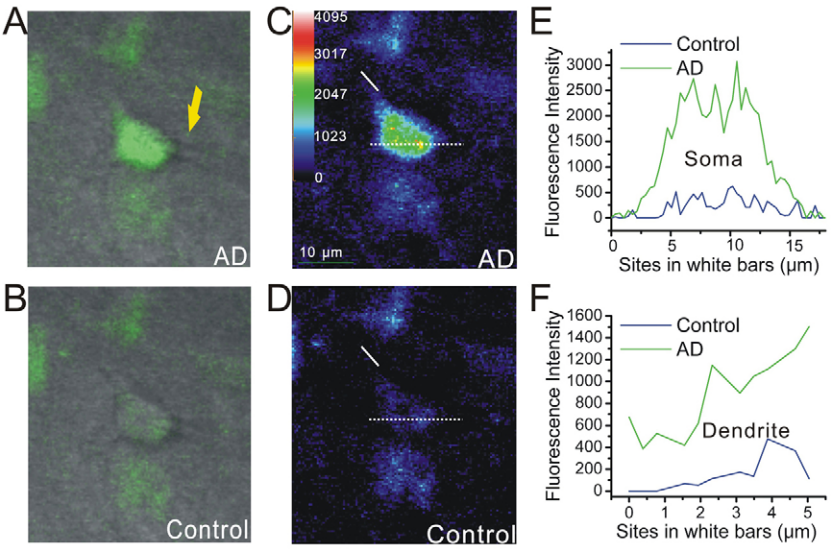

Fig. 1. Intracellular Ca^{2+} is increased by the infusion of adenophostin-A into pyramidal neurons. Adenophostin-A (AD) perfusion was carried out in a recording pipette (yellow arrow in A), which contained 100 nM AD. Ca^{2+} imaging was done as a control when the pipette had a cell-attached configuration on this pyramidal neuron. Suction was then added to produce whole-cell configuration. Immediately after whole-cell recording, we undertook Ca^{2+} imaging every 10 seconds. Superimposed image of pyramidal neurons under IR-DIC and Fluo-3-AM optics during AD perfusion (A) and in the control (B). Ca^{2+} transient in pyramidal neurons during AD perfusion (C) and under control (D), in which fluorescent intensities along white bars (solid line, dendrite; dotted line, soma) are measured for data presented in E,F. Ca^{2+} transient in the soma (E) and dendrite (F) of pyramidal neurons under AD perfusion (green line) and in the control (blue line).

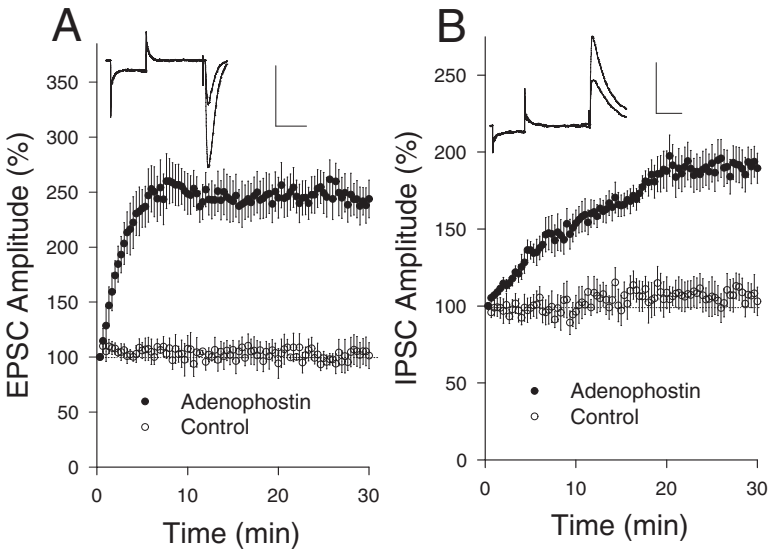

Fig. 2. The elevation of intracellular Ca^{2+} enhances glutamatergic and GABAergic synaptic transmission. (A) Elevation of cytoplasmic [Ca^{2+}] by infusing adenophostin-A into the neurons increases the amplitude of glutamatergic EPSCs (●) by ~145% compared with that in the control (○). Inset shows enhanced EPSC waveforms. (B) The intracellular infusions of adenophostin-A raise the amplitude of GABAergic IPSCs (●) by ~85% compared with controls (○). Inset shows IPSC waveforms. Glutamatergic EPSCs were isolated by using 10 μM bicuculline, whereas GABAergic IPSCs were isolated by adding 10 μM CNQX and 40 μM DAP-5.

adenophostin-A infusion (filled symbols). Despite the weak effect on the absolute RP_1 (triangles in Fig. 4B; P=0.81), an elevation of cytoplasmic [Ca^{2+}] prolonged the absolute RP_3 significantly (diamonds; P<0.01, n=12).

The effect of intracellular [Ca^{2+}] on V_{ts} is illustrated in Fig. 4C. When Ca^{2+} levels were raised by adenophostin-A, the V_{ts} values of spike 1 to spike 5 (V_{ts1}–V_{ts5}) shifted away from the resting membrane potential (V_r). The differential values (V_{ts}–V_r) for V_{ts1}, V_{ts2}, V_{ts3}, V_{ts4} and V_{ts5} were 19.7±0.73, 26.76±1.1, 27.44±1.18, 27.4±1.23 and 27.42±1.2 mV in the controls (open symbols), and 21.5±0.9, 30.84±1.3, 31.33±1.4, 31.5±1.46 and 31.8±1.44 mV after adenophostin-A infusion (filled symbols), respectively. V_{ts}–V_r values for corresponding spikes under both conditions were statistically different (P<0.01, n=12). The results above indicate that the elevation of cytoplasmic [Ca^{2+}] lowers spike capacity through increasing V_{ts} and prolonging RP.

An increase of V_{ts}–V_r lowers the sensitivity of neurons to synaptic inputs, and an increase in RP delays spiking, which downregulates the encoding of sequential spikes. However, Ca^{2+}-induced potentiation at excitatory and inhibitory synapses (Fig. 2) counteracts this downregulation because strong depolarization shortens the RP and hyperpolarization lowers the V_{ts} (Chen et al., 2006b; Chen et al., 2006c). We further investigated how Ca^{2+}-induced synaptic potentiation and somatic weakness interact to maintain homeostasis in neuronal spike encoding.

Ca^{2+}-induced plasticity at synapses and soma improves neuronal encoding

It is technically difficult to simultaneously record the activity of glutamatergic/GABAergic synapses and neurons in a single experiment. We therefore investigated the integrative influence of plasticity among those three compartments on spike encoding by using mixed pulses of strong depolarization and hyperpolarization, which mimic potentiation at excitatory and inhibitory synapses, and by using the current pulses mathematically integrated from glutamatergic/GABAergic synaptic potentiation

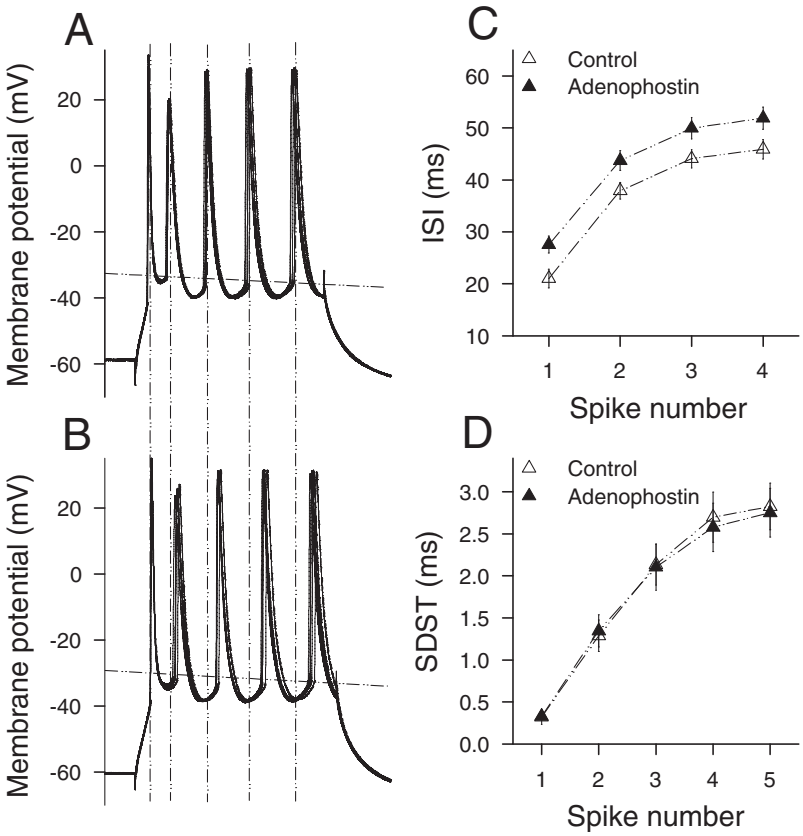

Fig. 3. The elevation of intracellular Ca^{2+} reduces spike capacity but not precision in cortical regular-spiking neurons. Superimposed waves of spikes under control (A) and adenophostin-A (B) infusion. Vertical lines are spike-locking phases, and horizontal lines are threshold potentials (V_{ts}). (C) The inter-spike interval (ISI) of sequential spikes under control (△) and adenophostin-A (▲) infusion, in which ISI values relevant to the same number in sequential spikes are statistically different (P<0.01). (D) The standard deviation of spike timing (SDST) under control (△) and adenophostin-A (▲) infusion.

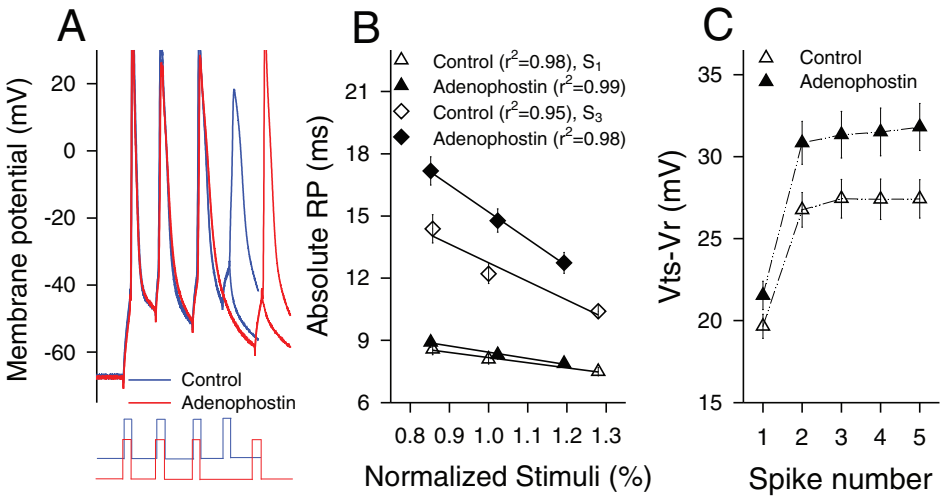

Fig. 4. The elevation of intracellular Ca^{2+} raises the V_{ts} and prolongs the RP of sequential spikes in regular-spiking neurons. (A) The superimposed waves of measuring absolute RP for spike 3 under control (blue traces) and adenophostin-A (red traces) infusion, where the absolute RP is defined as the duration from a complete spike to a subsequent spike evoked with 50% probability. (B) The relationship between the normalized stimuli and the absolute RP of spike 1 (S_1, triangles) or spike 3 (S_3, diamonds) under control (open symbols) and adenophostin-A (filled symbols) infusion, in which linear correlations are shifted upward. Values of the absolute RP-3 relevant to the similar stimulus intensity are statistically different ($P<0.01$). (C) The difference between V_{ts} and V_r ($V_{ts}–V_r$) for spike 1 to spike 5 under control (△) and adenophostin-A (▲) infusion, where V_{ts} values relevant to the same number in sequential spikes are statistically different ($P<0.01$).

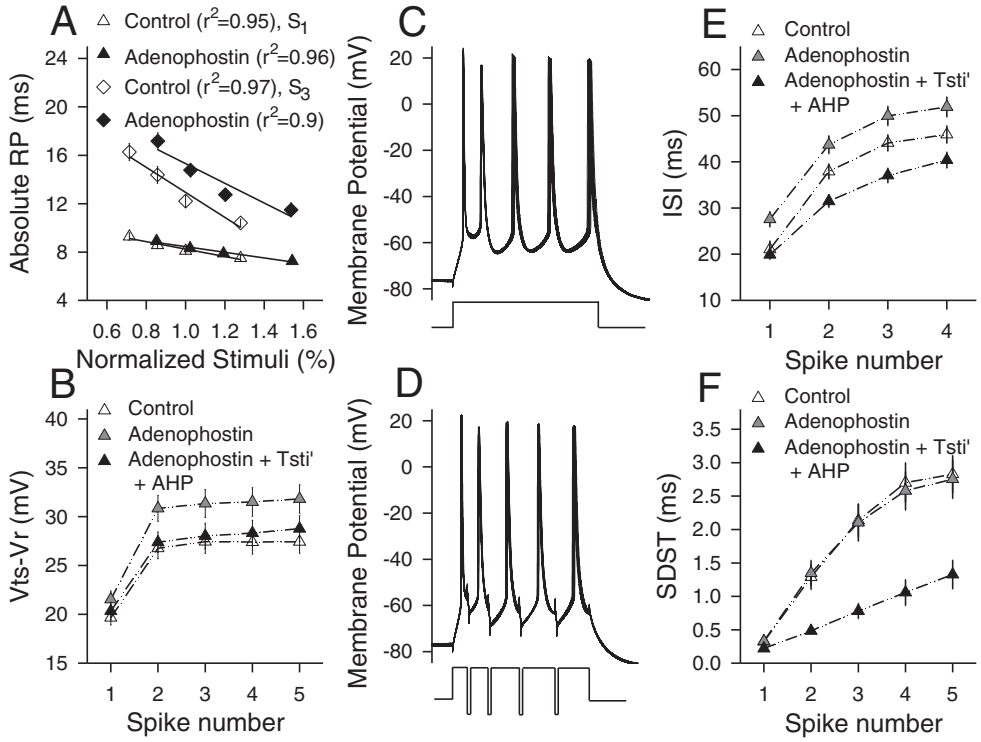

Fig. 5. Ca^{2+}-induced potentiation of excitatory and inhibitory synaptic transmission improves spike capacity and timing precision. Effect of intracellular Ca^{2+}-induced synaptic potentiation on spike encoding and neuronal intrinsic properties. The potentiation of excitatory and inhibitory synaptic inputs was mimicked by strong depolarization and hyperpolarization pulses. Data were obtained under control conditions (△), adenophostin-A infusion alone (gray triangles) or adenophostin-A together with strong depolarization (new threshold stimuli, Tsti') and AHP (▲). (A) Strong depolarization pulses reduce adenophostin-A-induced prolongation of the absolute RP. There is no statistical difference between adenophostin-A-treated (▲) and control (△) RPs in spike 1; however, a difference was observed with spike 3 for adenophostin-A infusion alone versus control (◆ versus ◇, respectively). (B) The mixture of strong depolarization/AHP pulses lowers adenophostin-raised $V_{ts}–V_r$ (▲) compared with that recorded with adenophostin-A alone (gray triangles, $P<0.05$). (C) Spike waveforms superimposed from 20 traces with adenophostin-A treatment alone. (D) Waveforms from 20 traces under adenophostin-A infusion with strong depolarization and AHP. (E) ISI values for corresponding spikes 2-4 between the three conditions are statistically different ($P<0.01$). (F) SDST values for spikes 2-5 under strong depolarization and AHP are significantly different ($P<0.01$) to those in adenophostin-A-treated and control.

(see Materials and Methods) during cellular infusion with adenophostin-A.

The influence of synaptic potentiation on neuronal programming

Current pulses consist of five pairs of alternative depolarization and afterhyperpolarization (AHP) pulses (Fig. 5D). Pulse intensities are set based on the threshold stimulus of somatic spikes, the strength of glutamatergic and GABAergic synapses under control conditions and Ca^{2+}-induced changes. AHP pulses (3 mseconds) are given based on the fact that inhibitory components after spikes are produced by feedback-inhibitory synapses (Sik et al., 1994; Freund and Buzsaki, 1996; McBain and Fisahn, 2001; Gutierrez, 2005) and/or fast AHP (Johnston et al., 2000).

The enhanced excitatory inputs decrease the Ca^{2+}-induced prolongation of RPs. Fig. 5A shows that linear correlations between the absolute RP and normalized stimuli were shifted down and towards the right compared with results in Fig. 4B. Values of absolute RP_1 were 9.28±0.3, 8.57±0.27, 8.1±0.24 and 7.5±0.2 mseconds under four control stimuli (△) and 8.9±0.3, 8.3±0.2, 7.88±0.2 and 7.24±0.2 mseconds under enhanced excitatory inputs (▲). Values of absolute RP_3 were 16.27±0.7, 14.38±0.68, 12.2±0.5 and 10.4±0.3 mseconds under four control stimuli (◇), and 17.17±0.67, 14.8±0.56, 12.74±0.5 and 11.5±0.6 mseconds under enhanced excitatory inputs (◆). The absolute RP values under these two conditions were not statistically different ($P>0.1$, $n=12$). The rise in cytoplasmic [Ca^{2+}] prolonged the absolute RP in the late phase of sequential spikes (Fig. 4A-B) and enhanced excitatory synaptic inputs (Fig. 2A) that shorten the absolute RP (Fig. 5A), indicating that the interaction of Ca^{2+}-induced changes between synapses and soma does not change spike RPs.

Fig. 5B shows that a combination of strong depolarization and AHP pulses decreased Ca^{2+}-raised V_{ts}. The values of V_{ts}–V_r for V_{ts1}, V_{ts2}, V_{ts3}, V_{ts4} and V_{ts5} were 19.7±0.73, 26.76±1.1, 27.44±1.18, 27.4±1.23 and 27.42±1.2 mV in the control (△); 21.53±0.86, 30.84±1.3, 31.33±1.4, 31.5±1.46 and 31.8±1.44 mV with adenophostin-A infusion (gray triangles); and 20.3±0.9, 27.4±1.1, 28±1.3, 28.3±1.3 and 28.76±1.31 mV with mixed pulses plus adenophostin-A infusions (▲). The value of V_{ts}–V_r for corresponding spikes was significantly lower with adenophostin-A and a mixed pulse than with adenophostin-A alone ($P=0.042$, $n=12$). This result indicates that the potentiation at glutamatergic and GABAergic synapses increases the sensitivity of neurons to excitatory inputs.

We further examined the influence of intracellular Ca^{2+} on ISI and SDST when applying the mixed pulses. Fig. 5E shows that the adenophostin-A infusion plus mixed pulses reduced Ca^{2+}-induced prolongation of ISI to levels below the control. The values of ISI_1, ISI_2, ISI_3 and ISI_4 were 21±1.8, 37.9±1.6, 44.1±1.8 and 45.9±1.9 mseconds for controls (△); 27.57±1.6, 43.72±1.9, 49.96±2.1 and 51.9±2.14 mseconds for adenophostin-A infusion (gray triangles); and 19.92±1, 31.48±1.37, 37.1±1.6 and 40.4±1.7 mseconds for mixed pulses plus adenophostin-A infusion (▲). ISI values for corresponding spikes from adenophostin-A infusion compared with mixed pulse plus adenophostin-A were significantly different ($P<0.01$, $n=12$).

Fig. 5F shows SDST changes by infusing adenophostin-A plus the mixed pulses. The values for $SDST_1$, $SDST_2$, $SDST_3$, $SDST_4$, $SDST_5$ were 0.32±0.1, 1.29±0.2, 2.14±0.24, 2.7±0.3 and 2.83±0.28 mseconds for controls (△); values were 0.33±0.03, 1.35±0.2, 2.1±0.3, 2.58±0.3 and 2.75±0.29 mseconds for adenophostin-A alone (gray triangles); and 0.22±0.04, 0.48±0.05, 0.78±0.11, 1.06±0.19 and 1.33±0.21 mseconds for mixed pulses plus adenophostin-A infusion (▲). Values from $SDST_2$ to $SDST_5$ for corresponding spikes under the last two conditions were statistically different ($P<0.01$, $n=12$). Although elevating Ca^{2+} levels alone did not change SDST (Fig. 3D and Fig. 5F), Ca^{2+}-induced potentiation at both excitatory and inhibitory synapses improved spike-timing precision.

These results indicate that Ca^{2+}-induced potentiation at excitatory and inhibitory synapses counterbalances Ca^{2+}-induced increases in V_{ts} and RP to improve spike capacity and timing precision. To further test this hypothesis, we used the pulses integrated mathematically from adenophostin-A-enhanced glutamatergic/GABAergic synaptic currents.

Effect of the pulses integrated from enhanced EPSPs and IPSPs on neuronal programming

The mathematical integration of excitatory and inhibitory synaptic inputs by a Metlab program (MathWorks) is based on a number of factors. (1) Transmission patterns at unitary glutamatergic synapses of each neuron fluctuate among facilitation, depression and parallel; GABAergic synapses are depressed in response to presynaptic sequential spikes in the control. (2) Glutamatergic and GABAergic synapses are upregulated and converted to a depression pattern by raising cytoplasmic [Ca^{2+}] (our unpublished data). (3) Presynaptic neurons are activated non-synchronously (Chen et al., 2006a). With such considerations, mathematical integration of

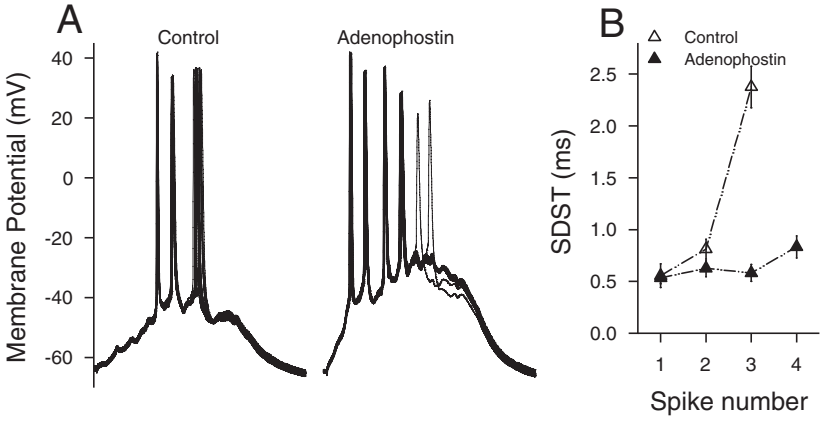

Fig. 6. The current pulses integrated from Ca^{2+}-induced potentiation at glutamatergic and GABAergic synapses improve spike encoding. (A) Superimposed waveforms of spikes evoked by currents integrated from GABAergic and glutamatergic synaptic transmission in the control (left panel) and with adenophostin-A-induced synaptic potentiation (right). The integrative effect of adenophostin-A on neuronal encoding is an increase in the number of sequential spikes. (B) SDST values of sequential spikes under control and adenophostin-A infusion, in which SDST is significantly different for spike 3 ($P<0.01$).

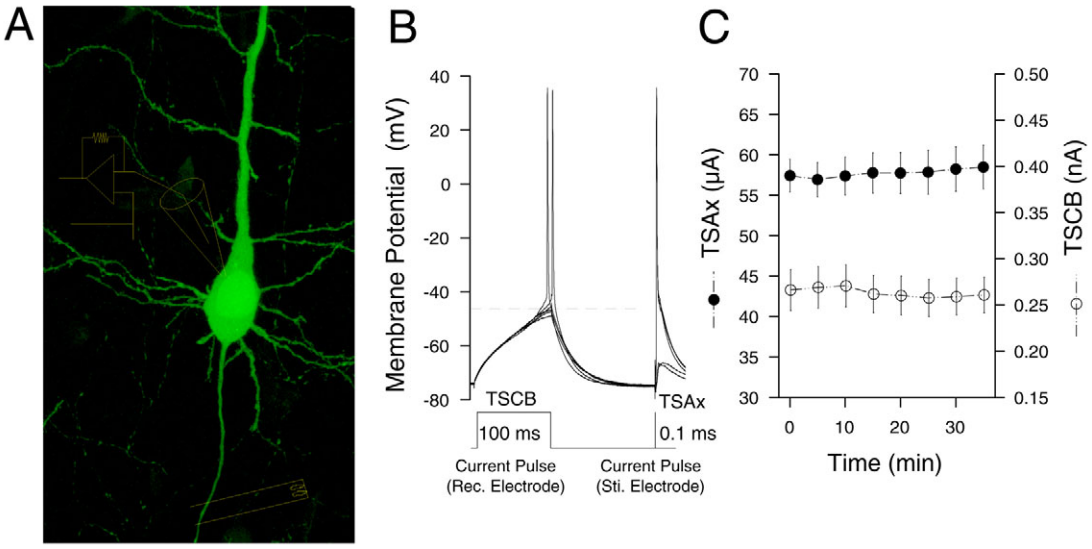

Fig. 7. The excitability of cell body and axon measured at cortical pyramidal neurons. (A) Tungsten electrodes at an axon output electrical pulses (0.1 mseconds) to evoke axonal excitation. A whole-cell pipette at the soma injects depolarization pulses (100 mseconds) to excite the neuron, and records electrical signal from soma and axon. (B) Threshold stimulation to the cell body or the axon (TSCB or TSAx, respectively) evoke single spikes at soma (left) and axon (antidromic, right) with 50% probability, which measure subcellular excitability. (C) TSAx and TSCB do not change over 35 minutes of recording (n=14).

glutamatergic versus GABAergic inputs were conducted in control conditions and after adenophostin-A infusion.

Fig. 6 shows the effects of current pulses integrated after 100 nM adenophostin-A infusion on spike encoding compared with controls. The current pulses in the controls evoked three spikes (left panel in Fig. 6A); whereas the current pulses under adenophostin-A-induced potentiation of glutamate/GABA synapses evoked more spikes with the forwarded spiking phases (right panel in Fig. 6A). In the quantitative data of Fig. 6B, the values of $SDST_1$–$SDST_3$ for control (open symbols) were 0.56±0.11, 0.81±0.094 and 2.38±0.2 mseconds; values $SDST_1$–$SDST_4$ for adenophostin-A infusion experiments (filled symbols) were 0.54±0.06, 0.63±0.08, 0.58±0.08 and 0.83±0.11 mseconds. $SDST_3$ values under these two conditions were statistically different (P<0.001, n=14). This result supports the results from in Fig. 5, which show that Ca^{2+}-induced potentiation at glutamatergic and GABAergic synapses counterbalances the Ca^{2+}-induced increase in somatic V_{ts} and RP to improve neuronal spike programming.

Homeostatic plasticity occurs between axons and soma

If the balance between dendritic synapses and soma is incomplete, an additional mechanism to maintain neuronal homeostasis is needed. We examined whether inverse plasticity occurs between somatic and axonal excitability. Tungsten electrodes were used to produce current pulses (0.1 mseconds) to activate axons. Whole-cell patch pipettes were used to inject depolarization pulses

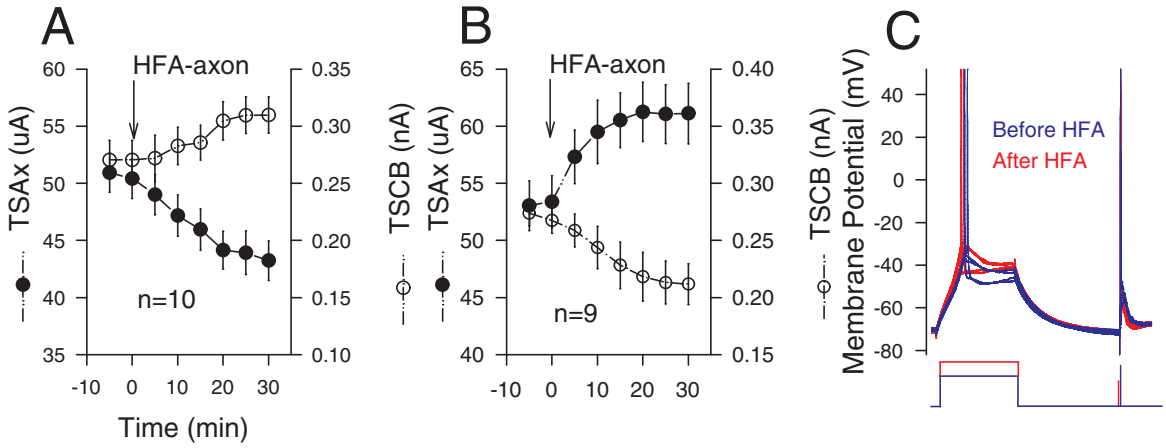

Fig. 8. Intensive activity at axons induces inverse changes in axonal and somatic excitability. (A) Axonal HFA lowers threshold stimuli at axons (TSAx, ●) and raises threshold stimuli at cell bodies (TSCB, ○; n=10). (B) Axonal HFA increases TSAx (filled symbols) and decreases TSCB (open symbols; n=9). (C) Single spikes elicited by threshold stimuli (50% probability of spike firing) at axons (right) and soma (left) before (blue traces) and after HFA (red traces). TSCB rises and TSAx is reduced after axonal HFA.

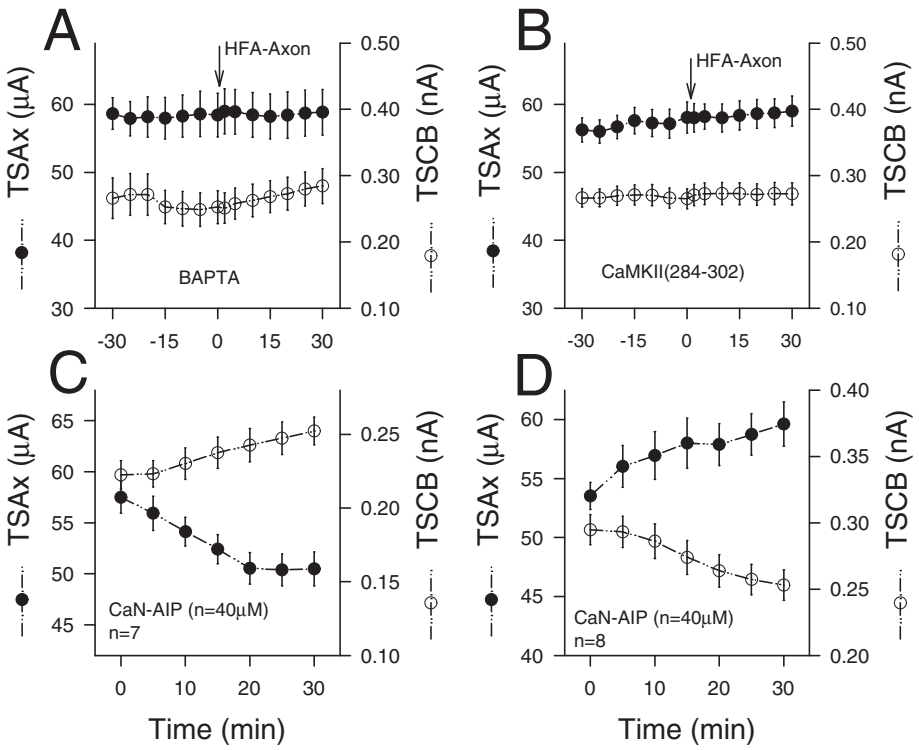

Fig. 9. Intracellular Ca^{2+} signaling pathways are essential to the inverse plasticity of axonal and somatic excitability induced by axonal HFA. BAPTA, CaMK(284-302) and CaN autoinhibitory peptide (CaN-AIP) were infused into the neurons via the recording pipette. (A) BAPTA prevents axonal HFA-induced plasticity of excitability dissociated at axons (●) and soma (○, *n*=8). (B) CaMK(284-302) blocks the inverse plasticity of axonal (●) and somatic excitability (○, *n*=11). (C) CaN-AIP lowers threshold stimuli at the axon (TSAx, ●) and raises threshold stimuli at cell body (TSCB, ○; *n*=7). (D) CaN-AIP increases TSAx (●) and decreases TSCB (○; *n*=8). All results are means ± s.e.m.

(10 mseconds) into the soma, and to record the excitation generated at the soma (left panel in Fig. 7B) and the axon (antidromic action potentials, right part). Their excitability was assessed by measuring threshold stimulus (TS) at the axon (TSAx) or cell body (TSCB) to evoke single spikes at the probability of 50% (Fig. 7B). With standard pipette solution (controls), we did not observe any significant change in TSAx (filled symbols) or TSCB (open symbols in Fig. 7C) for more than 35 minutes (*n*=14).

We then evoked antidromic spike bursts by giving five current pulses (0.1 mseconds, 20% above TSAx and 100 Hz) a total of 20 times to the axons. High frequency activity (HFA) at the axons variably altered the excitability among the neurons and their subcellular regions (Fig. 8). In 10 neurons (Fig. 8A), axonal HFA decreased TSAx from 50.9±1.7 to 43.2±1.7 μA (●; $P<0.01$), and increased TSCB from 0.27±0.017 to 0.31±0.016 nA (○; $P<0.01$). In nine neurons (Fig. 8B), HFA raised TSAx from 53.1±2.2 to 61.1±2.6 μA (●; $P<0.01$), and lowered TSCB from 0.27±0.011 to 0.21±0.017 nA (○; $P<0.01$). An example in Fig. 8C illustrates the spikes elicited by TSAx (right) and TSCB (left) before (blue traces) and after HFA (red traces). In four cells, HFA did not alter their excitability significantly. Intensive activity at the axons inversely shifted somatic and axonal excitability in two groups of cortical pyramidal neurons.

Axonal HFA probably activates voltage-gated Ca^{2+} channels (Tsien et al., 1988; Fisher et al., 1990) and raises Ca^{2+} in cells (Ehlers and Augustine, 1999; Liljelund et al., 2000). We examined the involvement of intracellular Ca^{2+} signals in HFA-induced inverse plasticity of axonal versus somatic excitability by infusing 1 mM BAPTA (a Ca^{2+} chelator) into the neurons. HFA was initiated at the axons 30 minutes after the infusion. Before and 30 minutes after HFA, TSAx values were 58.4±3.2 and 58.8±3.3 μA (filled symbols; *n*=8, *P*=0.91); and TSCB values were 0.25±0.023 and 0.28±0.026 nA (open symbols in Fig. 9A; *n*=8, *P*=0.78), respectively. These results indicate that the inverse plasticity of axonal and somatic excitability requires an increase in intracellular [Ca^{2+}].

An increased [Ca^{2+}] may change the active ratio of Ca^{2+}-dependent protein kinases (CaMK) to calcineurin (CaN). We examined whether this mechanism mediates inverse plasticity at the soma versus axons by infusing the autoinhibitory peptides (CaN-AIP and CaMK-AIP) into the neurons. We shifted the ratio toward dominant CaN activity by infusing 100 μM CaMKII(284-302) (Schulman and Lou, 1989). This infusion did not influence axonal and somatic excitability (–30 to 0 minutes in Fig. 9B), but prevented the effect of axonal HFA on their excitability. Before and 30 minutes after axonal HFA, TSAx values were 58.1±2.3 and 59.1±2.2 μA (●; *n*=11, *P*=0.89); and TSCB values were 0.265±0.015 and 0.27±0.016 nA (○ in Fig. 9B; *n*=11, *P*=0.81). Then we shifted their ratio toward dominant CaMKs activity by infusing 40 μM CaN-AIP (Hashimoto et al., 1990). This manipulation induced a similar effect to that of axonal HFA. In seven cells (Fig. 9C), CaN-AIP lowered TSAx from 57.5±1.5 to 50.5±1.6 μA (filled symbols; $P<0.01$), and raised TSCB from 0.22±0.01 to 0.253±0.01 nA (open symbols; $P<0.01$). In eight neurons (Fig. 9D), HFA increased TSAx from 53.5±1.1 to 59.6±1.9 μA (filled symbols; $P<0.01$) and reduced TSCB from 0.30±0.01 to 0.25±0.01 nA (open symbols; $P<0.01$). These data indicate that CaMKs activity may inversely drive the plasticity of axonal and somatic excitability.

Discussion

With neurons as a cellular model, we investigated homeostatic processes and the primary coordinators. The elevation of cytoplasmic [Ca^{2+}], which triggers biochemical cascades (Fig. 1), initiates fast-developing plasticity among subcellular compartments, including potentiation at glutamatergic and GABAergic synapses (Fig. 2), increases in V_{ts} and RP of somatic spikes (Figs 3, 4) and the inverse plasticity of excitability between axon and soma (Figs

8, 9). The integrative effect of these types of plasticity on neuronal functions is homeostatic in nature, which maintains the stabilization of neuronal excitability, secures the loyalty of information flowing through the dendrite, soma and axon, and improves encoding of neuronal signals (spike timing precision and capacity, Figs 5, 6) in an emergency and in a coordinated manner. These types of rapid-onset homeostatic plasticity among subcellular compartments are triggered by changes in cytoplasmic [Ca^{2+}]. With Ca^{2+} as a primary coordinator, the plasticity at a neuronal compartment is followed by plastic changes around neighbouring compartments in a homeostatic manner, such that the functional state of the neurons is stabilized and the encoding of neuronal signals is improved quickly.

Chronic homeostatic plasticity (Ramakers et al., 1990; Van Den Pol et al., 1996; Desai et al., 1999a; Desai et al., 1999b; Burrone and Murthy, 2003; Ehlers, 2003; Perez-Otano and Ehlers, 2005) may compensate for the original change in a specific neural activity to slowly reach stabilization by initiating expression of genes and proteins. The neurons are overly active when initiative factors are removed (Desai et al., 1999a; Desai et al., 1999b). The delayed compensation and withdrawal over-activity were not seen with fast-onset Ca^{2+}-induced homoeostatic plasticity in subcellular compartments in our study, because their plasticity was initiated and removed by common coordinators without the need for gene expression. We suggest that the simultaneous shift in the functional state of subcellular compartments in the opposite direction is a rapid and efficient way to minimize the destabilization of signal programming during neural plasticity. This is supported by a report of synaptic homeostasis where an increased transmitter release is followed by a blockade of postsynaptic receptors at neuromuscular junctions (Frank et al., 2006).

After developmental maturation and learning experience, signal programming at the neurons and its transmission at the synapses become precise (Angulo et al., 1999; Hashimoto and Kano, 2005; Guan et al., 2006). The dedicated processing of these precise signals over time confers stabilization of neuronal activities, which is known as cellular memory. However, intense activity at the synapse (Bliss and Gardner-Medwin, 1973; Stanton and Sejnowski, 1989) and the neuron (Aizenmann and Linden, 2000; Armano et al., 2000; Daoudal and Debanne, 2003; Zhang et al., 2004) induces their plasticity. Either a potentiation or depression in the function of synapses and neurons may destabilize the outputs of neural networks (Turrigiano and Nelson, 2004). To have the dedicated and precise encoding of neuronal signals, this destabilization should be rapidly corrected by the emergence of homeostatic mechanisms among the subcellular compartments (Figs 2-5) in neurons (the potentiation at the soma is associated with a depression at its axon in one group of neurons, or with potentiation in another group, Figs 8, 9), as well as between regular-spiking and fast-spiking neurons in the cerebral cortex (Wang and Kelly, 2001; Chen et al., 2006a). Such cellular homeostasis maintains the fidelity and precise encoding of neural signals in the networks, which stabilizes information processing, storage and outputs.

Membrane property influences the propagation of synaptic signals from the dendrites to soma (Shepherd, 2005); however, our study indicates that the strength of synaptic inputs regulates the intrinsic properties of the cell membrane. An increase in excitatory synaptic strength shortens the RP of a spike (Fig. 4B); and an increase in inhibitory strength lowers V_{ts} (Fig. 5B). The shortening of RPs increases spike capacity and timing precision, and the lowering of V_{ts} enhances the sensitivity of neurons to excitatory input (Chen et al., 2001; Chen et al., 2006b; Chen et al., 2006c). Therefore, synaptic plasticity influences intrinsic membrane properties and in turn improves spike encoding. This point is supported by our data that intracellular Ca^{2+}-induced potentiation at glutamatergic/GABAergic synapses (Fig. 2) corrects Ca^{2+}-induced destabilization of neuronal excitability (Figs 3, 4) and improves neuronal encoding (Figs 5, 6).

In addition to securing neuronal homeostasis and improving spike encoding, the reset of membrane excitability between subcellular compartments (synapses, soma and axon) enriches the spatial patterns of neuronal computation. When axonal excitability rises, the lower excitability in the soma means that it becomes insensitive to synaptic inputs and downregulates spiking. When somatic excitability rises, lower excitability in the axon weakens its ability to encode output signals (Figs 8, 9). Similar changes can also be seen at the dendrites versus soma and the excitatory versus inhibitory synapses (Figs 2-4). This is an excitation-inhibition pattern for individual neurons to compute neural information. This pattern may be present in neural networks because an increase of

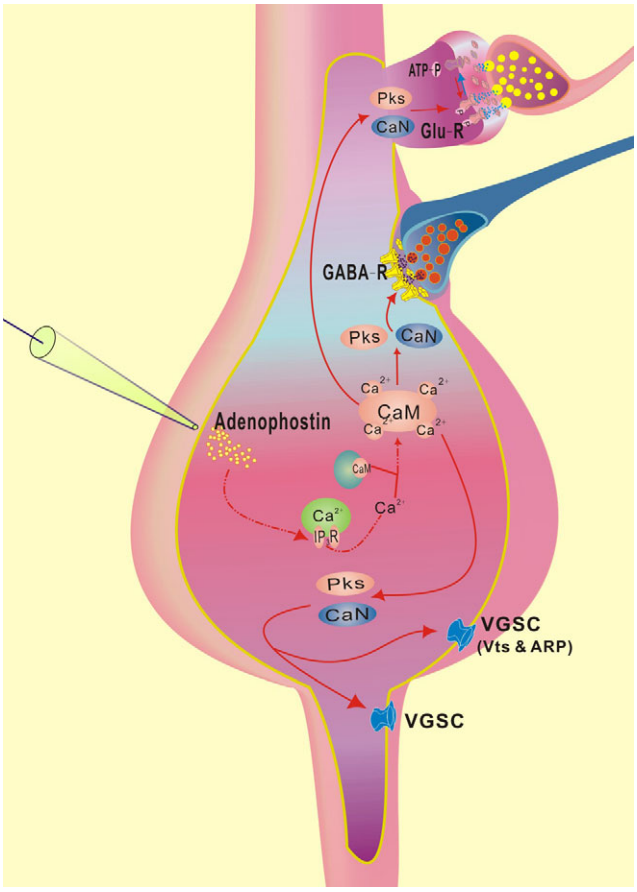

Fig. 10. Intracellular Ca^{2+}-signaling pathways induce plastic changes at subcellular compartments. The potentiation at the glutamatergic synapse enhances neuronal activity (red); the potentiation at the GABA synapse inhibits neuronal activity (blue); and the weakness in the soma (blue) is inversely associated with axonal potentiation (red), or vice versa. The integrated effects on neuronal programming are homeostatic in nature. ARP, absolute refractory period; CaM, calmodulin; CaN, calcineurin; GABA-R, GABA receptor; Glu-R, glutamine receptor; IP_3R, inositol (1,4,5)-trisphosphate receptor; Pks, protein kinases; VGSC, Voltage-gated sodium channel; Vts, threshold potential.

axonal excitability is associated with a decrease of somatic excitability in one group; however, the reverse situation occurs in another group. Considering the facts that membrane excitability varies among neurons (Zhang et al., 2004; Chen et al., 2006a) and that transmission patterns are different among synapses (Debanne et al., 1996; Reyes et al., 1998; Angulo et al., 1999; Reyes and Sakmann, 1999; Thomson and Bannister, 1999; Atzori et al., 2001; Rozov et al., 2001; Wang and Zhang, 2004), we suggest that the excitation-inhibition pattern among synapses, subcellular compartments and groups of neurons, which together constitute many well-organized societies in neural networks, is one of the essential processes in the computation of neural signals that encodes elegant brain functioning.

We show that increased cytoplasmic [Ca^{2+}] induces homeostatic plasticity among subcellular compartments: a new concept that cytoplasmic [Ca^{2+}] is a coordinator for homeostatic processes in the neuron. This expands previously published results on the role of Ca^{2+} in certain cellular events (Carafoli, 1987; Kennedy, 1989; Tsien and Tsien, 1990; Amundson and Clapham, 1993; Ehrlich, 1995; Ghosh and Greenberg, 1995; Berridge, 1998). Via protein kinases and phosphatases, Ca^{2+} regulates synaptic glutamine receptors and GABA receptors (Klee and Cohen, 1988; Huang, 1989; Kelly, 1992; McGlade-McCulloh et al., 1993; Krishek et al., 1994; Roche et al., 1994; De Koninck and Mody, 1996; Wang and Kelly, 1997) as well as voltage-gated Na^{+} channels (Catterall, 2000; Cantrell and Catterall, 2001). A coordinated change in kinetics allows the strength of synaptic transmission and the intrinsic properties of the neurons to maintain homeostatic plasticity in the subcellular compartments (illustrated in Fig. 10). It remains to be elucidated how the Ca^{2+}-signaling pathway differently regulates receptor channels and voltage-gated ion channels at subcellular locations (synapses, soma and axon) to rebalance the activities of these subcellular compartments, as well as how the coordination among these compartments develops. As the onset of homeostasis is so rapid, it is probably the presence of the functional redistribution of Ca^{2+}-dependent signaling molecules in subcellular compartments.

One could question whether other mechanisms elevating intracellular [Ca^{2+}], such as the intensive activation of mGluR1 and/or synapses, induce homeostatic plasticity. We have found similar results with adenophostin-A and high-frequency stimulus on synaptic potentiation (supplementary material Fig. S1), indicating that they both share similar mechanisms. In addition, intracellular [Ca^{2+}] rises when mGluR1 is activated by 50 μM (s)-3,5-dihydroxyphenylglycine (DHPG, supplementary material Fig. S2) or when synapses are activated intensively (supplementary material Fig. S3). We are investigating the influence of these manipulations on neuronal homeostasis. The increase in intracellular [Ca^{2+}] can vary among experimental treatments as well as between individual nerve cells. This may be due to a functional difference in the chemical reagents and treatments. For example, the infused adenophostin-A acts on all Ca^{2+} stores in a neuron, whereas HFS and DHPG act on synapse-associated Ca^{2+} stores. To study whether the plasticity in homeostatic nature occurs among subcellular compartments it is better to raise intracellular Ca^{2+} in all compartments of a cell, for which we used a potent and specific agonist of IP_3R (adenophostin-A) intracellularly to release Ca^{2+} from its stores in the whole cell. We are also examining whether different cells possess a mechanism to control intracellular Ca^{2+} levels quantitatively.

The plasticity at synapses and neurons is presumably a cellular model of learning and memory (Bliss and Collingridge, 1993; Wang et al., 1997). The major features after memory formation in animals include enhancement of working efficiency and regulation of behavior. The former can be explained by an increase in synaptic transmission and neuronal spike capacity. The behavioral regulation and stabilization are probably a result of the precise and dedicated output of signals from each neuron and bundle of neural networks. Therefore, the uniformity of synaptic patterns in transmitting sequential signals (Wang, J-H. et al., 2008), the improvement of spike timing precision (Figs 5, 6) and the homeostatic plasticity in subcellular compartments of individual neurons and subpopulations of neurons in neural networks, all stabilize signal encoding, which contributes to the consistent expression of neural information, i.e. memory.

We present a type of homeostatic plasticity with rapid onset in subcellular compartments (synapses, soma and axons), in which cytoplasmic Ca^{2+} signals are the primary coordinator. This homeostatic plasticity stabilizes neuronal excitability, improves spike encoding at the neurons and confers a spatial excitation-inhibition pattern for signal encoding in the neural networks. It is noteworthy that many cell types are asymmetrical in morphology and function. Whether these different cells maintain their homeostasis through the plasticity of subcellular compartments remains to be tested.

Materials and Methods

Brain slices

Cortical slices (400 μm) were prepared from Sprague-Dawley rats (postnatal day 18-22) that were decapitated after injection of pento-barbital (50 mg/kg). Slices were cut with a vibratome in modified and oxygenated (95% O_2, 5% CO_2) artificial cerebrospinal fluid (ACSF) (124 mM NaCl, 3 mM KCl, 1.2 mM NaH_2PO_4, 26 mM $NaHCO_3$, 0.5 mM $CaCl_2$, 5 mM $MgSO_4$, 10 mM dextrose and 5 mM HEPES, pH 7.35) at 4°C, and then were held in the normally oxygenated ACSF (124 mM NaCl, 3 mM KCl, 1.2 mM NaH_2PO_4, 26 mM $NaHCO_3$, 2.4 mM $CaCl_2$, 1.3 mM $MgSO_4$, 10 mM dextrose and 5 mM HEPES, pH 7.35) 24°C for 1-2 hours. One slice was transferred into a submersion chamber (Warner RC-26G) and perfused using normally oxygenated ACSF at 31°C for electrophysiological recording (Wang, 2003). Chemicals were from Sigma. The procedures were approved by IACUC in Beijing, China.

Neuron selection and whole-cell recording

Recordings were taken from neurons in layers IV and V of the sensorimotor cortex, in which regular spiking neurons show pyramidal-like soma and apical dendrites, by using a differential interference contrast (DIC) microscope (Nikon FN-E600). Electrical signals from the neurons were recorded by a multi-clamp 700B amplifier (Axon Instruments, Foster, CA) in current-clamp model for sequential spikes and voltage-clamp model for synaptic currents, and inputted into pClamp 9 (Axon Instruments) for data acquisition and analyses. The output bandwidth of amplifiers was set at 3 kHz. Instantaneous and steady-state currents evoked by hyperpolarization pulses of 5 mV (first part of the waves) were monitored and used to calculate the series and input resistance of cell membrane throughout each experiment to ensure recording quality. The spike patterns and modulation were studied by applying current pulses (depolarization, hyperpolarization or a mixture of both) and simulating pulses. GABAergic synaptic currents were isolated by using 40 mM D-AP5 and 10 mM CNQX, and glutamatergic synaptic responses were isolated by using 10 mM bicuculline. Tungsten electrodes (12 MΩ) were used to stimulate axons (Fig. 7A).

The standard pipette solution contained 150 mM potassium gluconate, 5 mM NaCl, 10 mM HEPES, 0.4 mM EGTA, 4 mM Mg-ATP, 0.5 mM Tris-GTP and 4 mM sodium phosphocreatine (pH 7.4 adjusted using 2M KOH). Fresh pipette solution was filtered using a 0.1 μm centrifuge filter before use. The osmolarity of the pipette solution was 295-305 mOsmol and the resistance was 6-8 MΩ. The intracellular infusions of signaling modulators (adenophostin-A and BAPTA from Sigma; CaN-AIP and CaMK-AIP from CalBiochem) were performed by back-filling the recording pipettes such that the data under the conditions of controls and agent treatments were obtained from the same neurons (Wang and Kelly, 2001). The success of such infusion was monitored by using Alexa Fluor 488, which can be seen in neurons around 3-4 minutes after whole-cell recording.

Neuronal intrinsic properties

The V_{ts} and RP of sequential spikes have been measured and defined in a previous study (Chen et al., 2006). Inter-spike interval (ISI) is the duration between a pair of spikes; and the SDST is the standard deviation of spike lock-phase. Spike thresholds

were also measured as threshold stimuli by injecting depolarization currents into the soma, and are defined as the minimal stimulus intensity of evoking a spike with 50% probability (Zhang et al., 2004). When studying homeostatic plasticity between an axon and the soma, the threshold stimuli of cell body (TSCB) for a single spike denotes somatic excitability. The threshold stimuli of axons (TSAx) for evoking a single antidromic spike (Fig. 7B, right panel) represents axonal excitability. The bursts of spikes (high-frequency activity, HFA) at axons were induced by giving a series of five 100 Hz current pulses (0.1 mseconds) whose intensity was 20% above the threshold stimuli, 20 times (350 msecond intervals).

Data were analyzed if membrane resting potentials (V_r) above –68 mV were recorded. The criteria for accounting data also included less than 5% changes in V_r, spike amplitude and input resistance in each experiment. The values of spike threshold, absolute RP, ISI and SDST are represented as the mean ± s.e.m. The statistical comparison of the data obtained under different conditions was done using the Student's *t*-test.

Integration of pulse waves from the summation of synaptic inputs

To integrate the pulses of hundreds of presynaptic inputs that are activated randomly, we assumed that presynaptic neurons (j=1, 2,…N) fire spikes at a specific rate, which evoke synaptic currents i (i.e. uEPSCs) in a postsynaptic neuron at times t_1, t_2,…t_n. The integrated currents (I) are described in equation 1. The integrated inputs are presumably correlated to uEPSCs linearly, in which $\alpha_j=(t/\tau)e^{-(t/\tau)}$ (Rall, 1967). α_j represents a single pulse that is inputted chronologically and decayed in a simply exponential manner:

$$I(t) = \sum_j \alpha_j (t - t_j) . \quad (1)$$

Equation 1 is a simple way to describe the characteristics of a low-pass filter in synaptic transmission, in which the currents are required to rise rapidly. In reality, the rising and decaying phases of synaptic currents develop slowly, and synapses are usually driven by two presynaptic spikes or even more. Therefore, we should apply the following equation to present two sequential synaptic responses:

$$\alpha_j = mte^{-\frac{t}{\tau}}\Theta(t) + n(t - T)e^{-\frac{(t-T)}{\tau}}\Theta(t - T) , \quad (2)$$

in which m and n are the amplitudes of uEPSC1 and uEPSC2, τ is the time constant, T is the interval between two pulses at a synapse and $\Theta(t)$ is the Heaviside step function with $\Theta(t)$=1 when t>0, and $\Theta(t)$=0 under other conditions.

The quantities of the parameters used to integrate current pulses from a population of glutamatergic and GABAergic unitary synapses are based on the following. (1) The spiking rate (F) of presynaptic neurons is 25 Hz. (2) They fire spikes asynchronously so that inter-input intervals are in the range of 0.35-1.85 mseconds. (3) adenophostin-A enhances EPSCs to ~243.8±17.2% and IPSCs to ~189.5±9.8% (Fig. 2), and Ca^{2+} signal converts the fluctuated transmission pattern into depression. (4) The number of synapses on a postsynaptic neuron is in the range of ~50-400; this number can be increased by a converting an inactive synapse into an active one. (5) The spectrum in the synchrony of presynaptic neurons is narrowed from 0.6-1.6 to 0.5-1.0 mseconds during the plasticity, which allows synaptic convergence more synchronously. The integration of events of unitary synapses was done using a programme written by us in Mat-lab.

Loading the Ca^{2+}-indicator Fluo-3-AM into neurons in brain slices

The acetoxymethyl (AM) ester of Ca^{2+} indicator (Fluo-3-AM) was dissolved in 20% Pluronic F-127 in DMSO for a stock solution of 1 mM, which was diluted in ACSF to the final concentration of 100 μM Fluo-3-AM. This loading solution was added into the slice-incubation chamber for 30 minutes, before it was washed out with oxygenated ACSF. For cellular imaging experiments, one brain slice was transferred to a submersion chamber and perfused with oxygenated ACSF at 2 ml/minute.

Cell imaging

Ca^{2+} imaging in pyramidal neurons was carried out using a confocal laser-scanning microscope (Olympus FV-1000, Olympus, Tokyo, Japan). A laser beam of 488 nm was used for Fluo-3-AM excitation. The scanning system was mounted onto an upright microscope (Olympus BX61WI) equipped with water-immersion objectives (↔40/0.8 NA). The average power delivered to brain slices was <10 mW. The parameters for the laser beam and the photomultiplier tube were locked throughout experiments for consistency before and after application of adenophostin-A, DHPG or high-frequency stimulus (100 Hz). Images were viewed and analyzed by using Fluoviewer. Data are presented as the change in fluorescence intensity.

The authors thank Sacha Nelson and Gina Turrigiano for the critical reading before submission, the JCS editorial office, Brian Lewis and Michelle Kirk for improving the final version, and Xin Zhou for laboratory assistance. This study was supported by National Awards for Outstanding Young Scientist (30325021), NSFC (30470362 and 30621130077), CAS Knowledge Innovation Program (KSCX2-YWR-39), National Basic Research Program (2006CB500804 and 2006CB911003) to J.-H.W.

References

Aizenmann, C. and Linden, D. J. (2000). Rapid, synaptically driven increases in the intrinsic excitability of cerebellar nuclear neurons. *Nat. Neurosci.* **3**, 109-111.

Amundson, J. and Clapham, D. (1993). Calcium waves. *Curr. Opin. Neurobiol.* **3**, 375-382.

Angulo, M. C., Staiger, J. F., Rossier, J. and Audinat, E. (1999). Developmental synaptic changes increase the range of integrative capabilities of an identified excitatory neocortical connection. *J. Neurosci.* **19**, 1566-1576.

Armano, S., Rossi, P., Taglietti, V. and D'Angelo, E. (2000). Long-term potentiation of intrinsic excitability at the mossy fiber-granule cell synapse of rat cerebellum. *J. Neurosci.* **20**, 5208-5216.

Atzori, M., Lei, S., Evans, L., Kanold, P. O., Phillips-Tansey, E., McIntyre, O. and McBain, C. J. (2001). Differential synaptic processing separates stationary from transient inputs to the auditory cortex. *Nat. Neurosci.* **4**, 1230-1237.

Berridge, M. J. (1998). Neuronal calcium signaling. *Neuron* **21**, 13-26.

Bliss, T. V. P. and Gardner-Medwin, A. R. (1973). Long-lasting potentiation of synaptic transmission in the dentate area of the unanaesthetized rabbit following stimulation of the perforant path. *J. Physiol. Lond.* **232**, 357-374.

Bliss, T. V. P. and Collingridge, G. L. (1993). A synaptic model of memory: LTP in the hippocampus. *Nature* **361**, 31-39.

Burrone, J. and Murthy, V. (2003). Synaptic gain control and homeostasis. *Curr. Opin. Neurobiol.* **13**, 560-567.

Burrone, J., O'Byrne, M. and Murthy, V. N. (2002). Multiple forms of synaptic plasticity triggered by selective suppression of activity in individual neurons. *Nature* **420**, 414-418.

Cantrell, A. R. and Catterall, W. A. (2001). Neuromodulation of Na+ channels: an unexpected form of cellular plasticity. *Nat. Rev. Neurosci.* **2**, 397-407.

Carafoli, E. (1987). Intracellular calcium homeostasis. *Annu. Rev. Biochem.* **56**, 395-433.

Catterall, W. A. (2000). From ionic currents to molecular mechanisms: the structure and function of voltage-gated sodium channels. *Neuron* **26**, 13-25.

Chen, N., Chen, S. L., Wu, Y. L. and Wang, J.-H. (2006a). The refractory periods and threshold potentials of sequential spikes measured by whole-cell recording. *Biochem. Biophys. Res. Commun.* **340**, 151-157.

Chen, N., Chen, X., Yu, J. and Wang, J.-H. (2006b). Afterhyperpolarization improves spike programming through lowering threshold potentials and refractory periods mediated by voltage-gated sodium channels. *Biochem. Biophys. Res. Commun.* **346**, 938-945.

Chen, N., Zhu, Y., Gao, X., Guan, S. and Wang, J.-H. (2006c). Sodium channel-mediated intrinsic mechanisms underlying the differences of spike programming among GABAergic neurons. *Biochem. Biophys. Res. Commun.* **346**, 281-287.

Chen, S., Gil, O., Ren, Y. Q., Zanazzi, G., Saizer, J. L. and Hillman, D. E. (2001). Neurotrimin expression during cerebellar development suggests roles in axon fasciculation and synaptogenesis. *Neurocytology* **30**, 927-937.

Correa, V., Riley, A. M., Shuto, S., Horne, G., Nerou, E. P., Marwood, R. D., Potter, V. L. and Taylor, C. W. (2001). Structural departments of adenophostin A activity at inositol triphosphate receptors. *Mol. Pharmacol.* **59**, 1206-1215.

Daoudal, D. and Debanne, D. (2003). Long-term plasticity of intrinsic excitability: learning rules and mechanisms. *Learn. Mem.* **10**, 456-465.

De Koninck, Y. and Mody, I. (1996). The effects of raising intracellular calcium on synaptic GABAA receptor-channels. *Neuropharmacology* **35**, 1365-1374.

Debanne, D., Guerineau, N. C., Gahwiler, B. H. and Thompson, S. M. (1996). Paired-pulse facilitation and depression at unitary synapses in rat hippocampus: quantal fluctuation affects subsequent release. *J. Physiol. Lond.* **491**, 163-176.

Delisle, S., Marksberry, E. W., Bonnett, C., Jenkins, D. J., Potter, B. V. L., Takahashi, M. and Tanzawa, K. (1997). Adenophostin A can stimulate Ca2+ influx without depleting the inositol 1,4,5,-triphosphate-sensitive Ca2+ stores in Xenopus Oocyte. *J. Biol. Chem.* **272**, 9956-9961.

Desai, N. S., Rutherford, L. and Turrigiano, G. G. (1999a). Plasticity in the intrinsic excitability of cortical pyramidal neurons. *Nat. Neurosci.* **2**, 515-520.

Desai, N. S., Rutherford, L. C. and Turrigiano, G. G. (1999b). BDNF regulates the intrinsic excitability of cortical neurons. *Learn. Mem.* **6**, 284-291.

Ehlers, M. D. (2003). Activity level controls postsynaptic composition and signaling via the ubiquitin-proteasome system. *Nat. Neurosci.* **6**, 231-242.

Ehlers, M. D. and Augustine, G. J. (1999). Cell signalling. Calmodulin at the channel gate. *Nature* **399**, 105-108.

Ehrlich, B. E. (1995). Functional properties of intracellular calcium-release channels. *Curr. Opin. Neurobiol.* **5**, 304-309.

Fisher, R. E., Gray, R. and Johnston, D. (1990). Properties and distribution of single voltage-gated calcium channels in adult hippocampal neurons. *J. Neurophysiol.* **64**, 91-104.

Frank, C. A., Kennedy, M. J., Goold, C. P., Marek, K. W. and Davis, G. W. (2006). Mechanisms underlying the rapid induction and sustained expression of synaptic homeostasis. *Neuron* **52**, 663-667.

Freund, T. F. and Buzsaki, G. (1996). Interneurons of the hippocampus. *Hippocampus* **6**, 347-470.

Ghosh, A. and Greenberg, M. E. (1995). Calcium signaling in neurons: molecular mechanisms and cellular consequences. *Science* **268**, 239-247.

Guan, S., Ma, S., Yan, Z., Ge, R., Wang, Q. and Wang, J. H. (2006). The intrinsic mechanisms underlying the maturation of programming sequential spikes at cerebellar Purkinje cells. *Biochem. Biophys. Res. Commun.* **345**, 175-180.
Gutierrez, R. (2005). The dual glutamatergic-GABAergic phenotype of hippocampal granule cells. *Trends Neurosci.* **28**, 297-303.
Hashimoto, K. and Kano, M. (2005). Postnatal development and synapse elimination of climbing fiber to Purkinje cell projection in the cerebellum. *Neurosci. Res.* **53**, 221-228.
Hashimoto, Y., Perrrino, B. A. and Soderling, T. R. (1990). Identification of an autoinhibitory domain in calcineurin. *J. Biol. Chem.* **265**, 1924-1927.
Huang, K. P. (1989). The mechanism of protein kinase C activation. *Trends Neurosci.* **12**, 425-432.
Johnston, D., Hoffman, D. A., Magee, J. C., Poolos, N. P., Watanabe, S., Colbert, C. M. and Migliore, M. (2000). Dendritic potassium channels in hippocampal pyramidal neurons. *J. Physiol. Lond.* **525**, 75-81.
Kelly, P. T. (1992). Calmodulin-dependent protein kinase II. *Mol. Neurobiol.* **5**, 153-177.
Kennedy, M. B. (1989). Regulation of neuronal function by calcium. *Trends Neurosci.* **12**, 417-420.
Klee, C. B. and Cohen, P. (ed.) (1988). The calmodulin-regulated protein phosphatase. In *Calmodulin* (*Molecular Aspects of Cellular Regulation*), pp. 225-248. Amsterdam: Elsevier.
Krishek, B. J., Xie, X.-M., Blackstone, C., Huganir, R. L., Moss, S. J. and Smart, T. G. (1994). Regulation of GABAA receptor function by protein kinase C phosphorylation. *Neuron* **12**, 1081-1095.
Liljelund, P., Netzeband, J. G. and Gruol, D. L. (2000). L-Type calcium channels mediate calcium oscillations in early postnatal Purkinje neurons. *J. Neurosci.* **20**, 7394-7403.
Lyncy, G., Larson, J., Kelso, S., Barrionuevo, G. and Schottler, F. (1983). Intracellular injections of EGTA block induction of hippocampal long-term potentiation. *Nature* **305**, 719-721.
McBain, C. J. and Fisahn, A. (2001). Interneurons unbound. *Nat. Rev. Neurosci.* **2**, 11-23.
McGlade-McCulloh, E., Yamamoto, H., Tan, S.-E., Brickey, D. A. and Soderlin, T. R. (1993). Phosphorylation and regulation of glutamate receptors by calcium/calmodulin-dependent protein kinase II. *Nature* **362**, 640-642.
Miller, R. J. (1991). The control of neuronal Ca2+ homeostasis. *Prog. Neurobiol.* **37**, 255-285.
Montell, C. (2005). The latest waves in calcium signaling. *Neuron* **122**, 157-163.
Neveu, D. and Zucker, R. S. (1996). Postsynaptic level of [Ca2+]i needed to trigger LTD and LTP. *Neuron* **16**, 619-629.
Perez-Otano, I. and Ehlers, M. D. (2005). Homeostatic plasticity and NMDA receptor trafficking. *Trends Neurosci.* **28**, 229-238.
Rall, W. (1967). Distinquishing theoretical synaptic potentials computed for different soma-dendritic distribution of synaptic inputs. *J. Neurophysiol.* **30**, 1138-1168.
Ramakers, G. J., Corner, M. A. and Habers, A. M. (1990). Development in the absence of spontaneous bioelectric activity results in increased stereotyped burst firing in cultures of associated cerebral cortex. *Exp. Brain Res.* **79**, 157-166.
Reyes, A. and Sakmann, B. (1999). Developmental switch in the short-term modification of unitary EPSPs evoked in layer 2/3 and layer 5 pyramidal neurons of rat neocortex. *J. Neurosci.* **15**, 3827-3835.
Reyes, A., Lujan, R., Rozov, A., Burnashev, N., Somogyi, P. and Sakmann, B. (1998). Target-cell-specific facilitation and depression in neocortical circuits. *Nat. Neurosci.* **1**, 279-285.
Roche, K. W., Tingley, W. G. and Huganir, R. L. (1994). Glutamate receptor phosphorylation and synaptic plasticity. *Curr. Opin. Neurobiol.* **4**, 383-388.
Rozov, A., Burnashev, B., Sakmann, B. and Neher, E. (2001). Transmitter release modulation by intracellular Ca2+ buffers in facilitating and depressing nerve terminals of pyramidal cells in layer 2/3 of the rat neocortex indicates a target cell-specific difference in presynaptic calcium dynamics. *J. Physiol. Lond.* **531**, 807-826.
Schulman, H. and Lou, L. L. (1989). Multifunctional Ca2+/calmodulin-dependent protein kinase: domain structure and regulation. *Trends Biochem. Sci.* **14**, 62-66.
Shepherd, G. M. (2005). *Information Processing in Complex Dendrites*. New York: Elsevier Academic Press.
Sik, A., Ylinen, A., Penttonen, M. and Buzsaki, G. (1994). Inhibitory CA1-CA3-hilar region feedback in the hippocampus. *Science* **265**, 1722-1724.
Stanton, P. K. and Sejnowski, T. J. (1989). Associative long-term depression in the hippocampus induced by hebbian covariance. *Nature* **339**, 215-218.
Takahashi, M., Tanzawa, K. and Takahashi, S. (1994). Adenophostins, newly discovered metabolites of Penicillium brevicompactum, act as potent agonist of inositol 1,4,5-triphosphate receptor. *J. Biol. Chem.* **269**, 369-372.
Thiagarajan, T. C., Piedras-Renteria, E. S. and Tsien, R. W. (2002). Alpha- and beta-CaMKII. Inverse regulation by neuronal activity and opposing effects on synaptic strength. *Neuron* **36**, 1103-1114.
Thomson, A. M. and Bannister, P. A. (1999). Release-independent depression at pyramidal inputs onto specific cell targets: dual recordings in slices of rat cortex. *J. Physiol. Lond.* **519**, 57-70.
Tsien, R. W. and Tsien, R. Y. (1990). Calcium channels, stores, and oscillations. *Annu. Rev. Cell Biol.* **6**, 715-760.
Tsien, R. W., Lipscombe, D., Madison, D. V., Bley, K. R. and Fox, A. P. (1988). Multiple types of neuronal calcium channels and their selective modulation. *Trends Neurosci.* **11**, 432-438.
Turrigiano, G. G. and Nelson, S. (2004). Homeostatic plasticity in the developing nervous system. *Nat. Rev. Neurosci.* **5**, 97-107.
Van Den Pol, A. N., Obrietan, K. and Belousov, A. (1996). Glutamate hyperexcitability and seizure-like activity throughout the brain and spinal cord upon relief from chronic glutamate receptor blockade in culture. *Neuroscience* **74**, 653-674.
Wang, J.-H. (2003). Short-term cerebral ischemia causes the dysfunction of interneurons and more excitation of pyramidal neurons. *Brain Res. Bull.* **60**, 53-58.
Wang, J.-H. and Stelzer, A. (1996). Shared calcium signaling pathways in the induction of long-term potentiation and synaptic disinhibition in CA1 pyramidal cell dendrites. *J. Neurophysiol.* **75**, 1687-1702.
Wang, J.-H. and Kelly, P. T. (1997). Postsynaptic calcineurin activity down-regulates synaptic transmission by weakening intracellular Ca2+ signaling mechanisms in hippocampal CA1 neurons. *J. Neurosci.* **17**, 4600-4611.
Wang, J.-H. and Kelly, P. T. (2001). Ca2+/CaM signalling pathway up-regulates glutamatergic synaptic function in non-pyramidal fast-spiking neurons of hippocampal CA1. *J. Physiol. Lond.* **533**, 407-422.
Wang, J.-H. and Zhang, M. (2004). Differential modulation of glutamatergic and cholinergic synapses by calcineurin in hippocampal CA1 fast-spiking interneurons. *Brain Res.* **1004**, 125-135.
Wang, J. H., Ko, G. and Kelly, P. T. (1997). Cellular and molecular bases of memory: synaptic and neuronal plasticity. *J. Clin. Neurophysiol.* **14**, 264-293.
Wang, J.-H., Wei, J., Chen, X., Yu, J., Chen, N. and Shi, J. (2008). Gain and fidelity of transmission patterns at cortical excitatory unitary synapses improve spike encoding. *J. Cell Sci.* **121**, 2951-2960.
Zhang, M., Hung, F., Zhu, Y., Xie, Z. and Wang, J. (2004). Calcium signal-dependent plasticity of neuronal excitability developed postnatally. *J. Neurobiol.* **61**, 277-287.